Title

Modeling of Store Gletscher's calving dynamics, West Greenland, in response to ocean thermal forcing

Journal

Geophysical Research Letters, 43(6)

ISSN

0094-8276

Authors

Morlighem, M
Bondzio, J
Seroussi, H
et al.

Publication Date

2016-03-28

DOI

10.1002/2016gl067695

Peer reviewed

AGU PUBLICATIONS

Geophysical Research Letters

RESEARCH LETTER
10.1002/2016GL067695

Key Points:
- Store is remarkably stable due to the presence of a sill in the vicinity of its front
- A quadrupling of ocean-induced melt is required to dislodge the glacier from its stabilizing sill
- A temporary increase in melting at the front can trigger a dramatic retreat of the glacier

Supporting Information:
- Supporting Information S1
- Movie S1
- Movie S2
- Movie S3
- Movie S4
- Movie S5
- Movie S6

Correspondence to:
M. Morlighem,
Mathieu.Morlighem@uci.edu

Citation:
Morlighem, M., J. Bondzio, H. Seroussi, E. Rignot, E. Larour, A. Humbert, and S. Rebuffi (2016), Modeling of Store Gletscher's calving dynamics, West Greenland, in response to ocean thermal forcing, *Geophys. Res. Lett.*, *43*, doi:10.1002/2016GL067695.

Received 6 JAN 2016
Accepted 20 FEB 2016
Accepted article online 25 FEB 2016

Modeling of Store Gletscher's calving dynamics, West Greenland, in response to ocean thermal forcing

M. Morlighem[1], J. Bondzio[1,2], H. Seroussi[3], E. Rignot[1,3], E. Larour[3], A. Humbert[2], and S. Rebuffi[1]

[1]Department of Earth System Science, University of California, Irvine, California, USA, [2]Alfred Wegener Institute, Helmholtz Centre for Polar and Marine Research, Bremerhaven, Germany, [3]Jet Propulsion Laboratory, California Institute of technology, Pasadena, California, USA

Abstract Glacier-front dynamics is an important control on Greenland's ice mass balance. Warmer ocean waters trigger ice-front retreats of marine-terminating glaciers, and the corresponding loss in resistive stress leads to glacier acceleration and thinning. Here we present an approach to quantify the sensitivity and vulnerability of marine-terminating glaciers to ocean-induced melt. We develop a plan view model of Store Gletscher that includes a level set-based moving boundary capability, a parameterized ocean-induced melt, and a calving law with complete and precise land and fjord topographies to model the response of the glacier to increased melt. We find that the glacier is stabilized by a sill at its terminus. The glacier is dislodged from the sill when ocean-induced melt quadruples, at which point the glacier retreats irreversibly for 27 km into a reverse bed. The model suggests that ice-ocean interactions are the triggering mechanism of glacier retreat, but the bed controls its magnitude.

1. Introduction

Realistic modeling of the Greenland ice sheet is essential to improve projections of its past, present, and future contributions to sea level rise in a warming climate [*Church et al.*, 2013]. The recent increase in the rate of mass loss from the Greenland ice sheet is in part due to the acceleration and thinning of outlet glaciers along the coast [e.g., *van den Broeke et al.*, 2009]. This acceleration is a dynamic response to the retreat of marine terminating glaciers, which leads to a loss in resistive stresses [e.g., *Howat et al.*, 2008]. As ocean waters that reach the glacier termini warm up and surface runoff increases, calving fronts are exposed to more ocean-induced melt [*Xu et al.*, 2013]. It is essential to assess the sensitivity of individual glaciers to enhanced melting to determine which are most likely to change over the coming decades and under which ocean thermal forcing. Addressing this question requires to use numerical models that have the ability to move the calving front dynamically and employ a proper parameterization of ocean-induced melt, sliding, and calving.

Today, the vast majority of ice sheet models that include moving boundaries are one-dimensional flow line and vertical flow band models [e.g., *Nick et al.*, 2013; *Todd and Christoffersen*, 2014]. These models are not adapted to the complex geometries of Greenland outlet glaciers, as they do not accurately capture changes in lateral stresses and fluxes. Moving boundaries have been used on plan view two-dimensional (2-D) models [*Albrecht et al.*, 2011; *Pollard and DeConto*, 2009], but only for Antarctic ice shelves.

Here we use the level set method [*Osher and Sethian*, 1988] to track moving boundaries within a 2-D plan view model part of the Ice Sheet System Model (ISSM) [*Larour et al.*, 2012; *Bondzio et al.*, 2016], and investigate the sensitivity of Store Gletscher's ice front position and velocity under different forcing scenarios. Store, in West Greenland, has not experienced any significant change over the past century and is one of the few outlet glaciers of Greenland for which quality bed topography and ocean bathymetry is available, which is critically important for modeling ice front dynamics.

To model the ice calving at the front of Store, we rely on a new calving law adapted from a von Mises yield criterion. We investigate the response of the glacier to the amount of melting occurring at its calving face to determine its sensitivity and vulnerability to climate forcing. We conclude on the sensitivity of Store to external forcings and how this approach could be used to other glaciers.

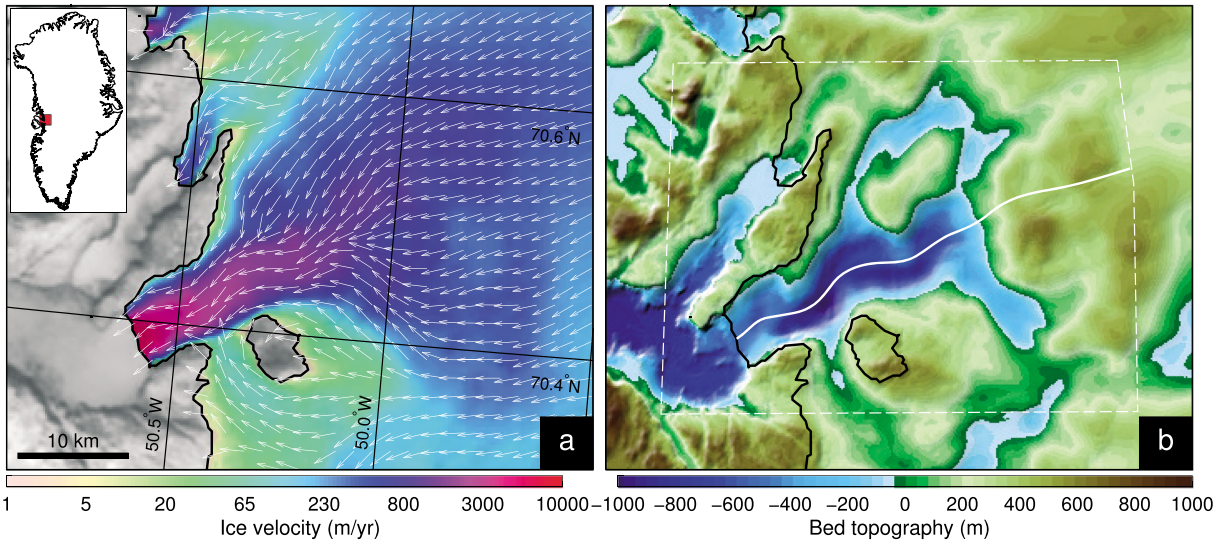

Figure 1. (a) InSAR-derived surface velocities of Store Gletscher [*Rignot and Mouginot*, 2012] and (b) bed topography inferred from mass conservation [*Morlighem et al.*, 2014] for grounded ice and multibeam echo sounding measurements in the fjord. The black line indicates the ice edge, the thin dashed white line is the model domain, and the white line is the flow line used in Figure 3.

2. Data and Method

2.1. Store Gletscher

Store Gletscher, or Store (70.4°N, 50.55°W), has been remarkably stable over the past century [*Weidick and Bennike*, 2007], both in terms of velocity and ice front position [*Rignot et al.*, 2015], possibly since the little ice age [*Weidick*, 1968]. Store flows along a valley that remains below sea level for about 60 km, and its ice front is resting on a sill that is ~450 m below sea level at a narrowing passage of the terminal valley [*Rignot et al.*, 2015; *Morlighem et al.*, 2014]. Downstream of the sill, the fjord is 700–800 m deep, and the bed upstream is retrograde and reaches a depth of 800 m (Figure 1b). The glacier flows at 6300 m/yr at the calving front and drains a catchment basin of 30,500 km^2 into the ocean [*Rignot and Mouginot*, 2012] (Figure 1a).

We have assembled a complete and high-resolution bed topography map, by combining the bed derived from mass conservation [*Morlighem et al.*, 2011] from BedMachine Greenland [*Morlighem et al.*, 2014] with multibeam echo sounding measurements in the fjord [*Rignot et al.*, 2015]. This map provides a seamless transition from the topography under the ice to the fjord bathymetry in front of the ice. The surface topography used to model the glacier is the Greenland ice mapping project digital elevation model [*Howat et al.*, 2014].

2.2. Level Set Method

Moving boundaries can be treated in an explicit form, represented by a set of segments that move between time steps or implicitly using, e.g., a level set method. The level set method has a number of advantages compared to an explicit method [*Osher and Sethian*, 1988; *Bondzio et al.*, 2016]. It is numerically more stable, does not require to remesh the model domain after each time step, and can deal with complex topological operations (such as splitting or merging ice streams).

The level set method consists in defining a scalar field, φ, whose zero contours define the position of the ice boundary:

$$\begin{cases} \varphi(\mathbf{x}, t) < 0 & \text{if } \mathbf{x} \text{ is in the ice at time } t \\ \varphi(\mathbf{x}, t) > 0 & \text{if } \mathbf{x} \text{ is not in the ice at time } t \\ \varphi(\mathbf{x}, t) = 0 & \text{if } \mathbf{x} \text{ is on the ice boundary at time } t \end{cases} \tag{1}$$

Here we initialize our level set function using a signed distance approach. $\varphi(\mathbf{x}, 0)$ is the distance between the point $\mathbf{x}$ and the initial ice front, and we multiply this distance by -1 if $\mathbf{x}$ is in the ice domain.

As the model evolves through time, we change the value of φ to adjust the model boundary. The boundary moves at a velocity:

$$\mathbf{v}_f = \mathbf{v} - \left(c + \dot{M}\right)\mathbf{n} \tag{2}$$

where $\mathbf{v}_f$ is the ice front velocity vector, $\mathbf{v}$ is the ice velocity vector at the ice front, c is the calving rate, $\dot{M}$ is the melting rate on the calving face, and $\mathbf{n}$ is a unit normal vector that points outward from the ice domain.

For each time step, we advect φ using the velocity $\mathbf{v}_f$ in order to simulate a change in model boundary:

$$\frac{\partial \varphi}{\partial t} = -\mathbf{v}_f \cdot \nabla \varphi \tag{3}$$

To avoid any distortion in the level set function, we reinitialize φ using the signed distance approach at each time step. *Bondzio et al.* [2016] provide a complete description of the implementation of the level set method in ISSM.

2.3. Calving Law

A calving law is included in this framework by specifying the governing equation of the calving rate, c. *Levermann et al.* [2012] proposed a calving speed proportional to the product of the strain rate along and across flow. Although this calving law seems well suited to Antarctic ice shelves, it does not work for Greenland's outlet glaciers that flow in narrow fjords. Along valleys with nearly parallel walls, the transverse component of the velocity is close to zero, and the transversal strain rate is therefore also close to zero and noisy.

Here we use a calving law based on tensile stresses as follows:

$$c = \|\mathbf{v}\| \frac{\tilde{\sigma}}{\sigma_{\max}} \tag{4}$$

where $\tilde{\sigma}$ is a scalar quantity representing the stress regime of the glacier, and $\sigma_{\max}$ is a threshold. In the absence of melt and assuming that the ice velocity is perpendicular to the ice front, the front of the glacier is stable if $\tilde{\sigma} = \sigma_{\max}$. If $\tilde{\sigma}$ exceeds the threshold, the ice front retreats ($c > \|\mathbf{v}\|$), and if $\tilde{\sigma}$ is below the threshold, the ice front advances ($c < \|\mathbf{v}\|$). To define $\tilde{\sigma}$, we use the von Mises stress. The von Mises yield criterion is one of the most widely used yield criteria in solid mechanics and structural analysis. Calving rate being primarily controlled by stretching [*Benn et al.*, 2007], the von Mises stress is the natural quantity to measure in order to assess the amount of fracturing, and hence the calving speed, in marine terminating glaciers. This criterion has also been used to model crevasses and fractures of ice shelves [e.g., *Vaughan*, 1993; *Albrecht and Levermann*, 2014] and mountain glaciers [e.g., *Hubbard et al.*, 1998].

For incompressible materials and using Glen's flow law, the von Mises stress is

$$\sigma_{\text{vm}} = \sqrt{\frac{3}{2} \sum_{i,j} \sigma'_{ij} \sigma'_{ij}} = \sqrt{3}\, B\, \dot{\varepsilon}_e^{1/n} \tag{5}$$

where σ'_{ij} is the (i, j) component of the deviatoric stress, $\dot{\varepsilon}_e$ is the effective strain rate, B is the ice viscosity parameter, and $n = 3$ is Glen's exponent. Because the ice tensile fracture strength is considerably smaller than its compressive fracture strength [*Benn et al.*, 2007], we define the effective tensile strain rate as

$$\tilde{\dot{\varepsilon}}_e^2 = \frac{1}{2} \left(\max\left(0, \dot{\varepsilon}_1\right)^2 + \max\left(0, \dot{\varepsilon}_2\right)^2 \right) \tag{6}$$

where $\dot{\varepsilon}_1$ and $\dot{\varepsilon}_2$ are the two eigenvalues of the 2-D strain rate tensor, so that only tensile deformation is accounted for ($\dot{\varepsilon}_1 > 0$ if the ice is stretching along the first principal direction). We define the tensile von Mises stress as

$$\tilde{\sigma} = \sqrt{3}\, B\, \tilde{\dot{\varepsilon}}_e^{1/n} \tag{7}$$

Additionally, we know that Store does not have a floating extension except on occasions [*Rignot et al.*, 2015]. In all our experiments, we force the glacier to calve when ice crosses hydrostatic equilibrium for the first time by explicitly changing the value of the level set in these regions.

2.4. Model Setup and Experiments

We rely on a 2-D plan view model and use the Shelfy-Stream Approximation [*MacAyeal*, 1989] to model Store Gletscher. The mesh has a resolution that varies between 100 m in the vicinity of the ice front and 1000 m inland and comprises about 30,000 elements. We apply water pressure at the ice-ocean interface, a stress-free boundary condition at the ice/air interface and constrain the model with interferometric synthetic aperture radar (InSAR)-derived velocities from 2007–2008 at the inflow boundary [*Rignot and Mouginot*, 2012].

We initialize the model by inverting for basal friction [*Morlighem et al.*, 2010, 2013] using InSAR-derived surface velocities and assume a viscosity equivalent to an ice temperature of −5°C using the table provided by *Cuffey and Paterson* [2010] because this temperature is consistent with the modeled steady state temperature of *Seroussi et al.* [2013].

As the model runs forward in time, we use a time step of 1 week and let the model run for 20 years. We employ a surface mass balance from the Regional Atmospheric Climate Model-2 [*van Angelen et al.*, 2014] and assume no melting at the base of grounded ice.

The melt rate at the calving face has a strong seasonal variability. Based on high-resolution ocean circulation model of this fjord, *Xu et al.* [2013] found that the melt rate varies from a few 10 cm/d in the winter to a maximum of 2–3 m/d in the summer. Oceanic measurements confirm this maximum summer melt rate [*Xu et al.*, 2013]. It is here parameterized as

$$\dot{M} = \dot{M}_{\max} \frac{(1 + \sin(2\pi t))}{2} \tag{8}$$

where $\dot{M}_{\max}$ is the maximum melt rate in the summer and t is the time in years, and our reference melt rate is $\dot{M}_{\max} = 3$ m/d to be consistent with *Xu et al.* [2013]. The melt rate is applied uniformly at the calving face when the bathymetry is greater than 300 m and is set to 0 in places where the bed is higher than sea level. A linear transition is applied between these two depths.

The only parameter that needs to be calibrated in the calving law is the stress threshold, $\sigma_{\max}$ (equation (4)). To calibrate this threshold, we let the model run for 20 years using our reference melt rate of $\dot{M}_{\max} = 3$ m/d using different values for $\sigma_{\max}$. For $\sigma_{\max} < 1$ MPa, the ice front retreats inland whereas $\sigma_{\max} > 1$ MPa yield to stable ice front positions. We would expect the ice front to advance for larger values of $\sigma_{\max}$, but if the ice front advances downstream of its sill, where the bathymetry is deeper, it forms a floating tongue that is instantly broken off by the model. We therefore set the stress threshold to $\sigma_{\max} = 1$ MPa. We find that this value is consistent with the range of ice tensile strengths (0.7 MPa to 3.1 MPa, less than 1.43 MPa for temperatures above −10°C) reported by *Petrovic* [2003].

We would like to assess how stable Store Gletscher is to an increase in ocean forcing, and more specifically, how stable its ice front is when the amount of melting occurring at its ice front, $\dot{M}$, changes. An increase in this melting rate could either be due to a change in advection of warm, salty, subsurface water toward the front, and/or to an increase in runoff production that enhances the circulation in the fjord [*Xu et al.*, 2013]. To address this question, we increase the summer melt, $\dot{M}_{\max}$, from 3 m/d to up to 12 m/d leaving all other model parameters constant in order to determine the threshold above which the glacier starts to retreat over our 20 year simulation.

3. Results

We first look at the unperturbed experiment, where the melt rate at the ice front is imposed as $\dot{M}_{\max} = 3$ m/d (Figure 2a, 3a, and Movie S1 in the supporting information). Over 20 years, we only see a minor adjustment of the ice front but no significant retreat or advance, and the velocity remains stable close to its current value. Most of the ice front adjustment takes place close to the southern side of the fjord. This is also a location where the misfit between the model and observed velocities is the largest. Our initial stress state is therefore not well estimated in this region, which may explain why our calving criterion leads to a small retreat of the front in this location. After 20 years, the glacier only gains about 3% of its initial volume (Figure1b), which is typical for model relaxation.

We then increase the applied melt rate to 6 m/d in the summer (Figures 2b and 3b), but this change does not affect the dynamics of the ice front, which converges to the same position as the one of the reference experiments. The seasonal cycle in the ice front position (Movie S2) is stronger, i.e., the glacier front retreats

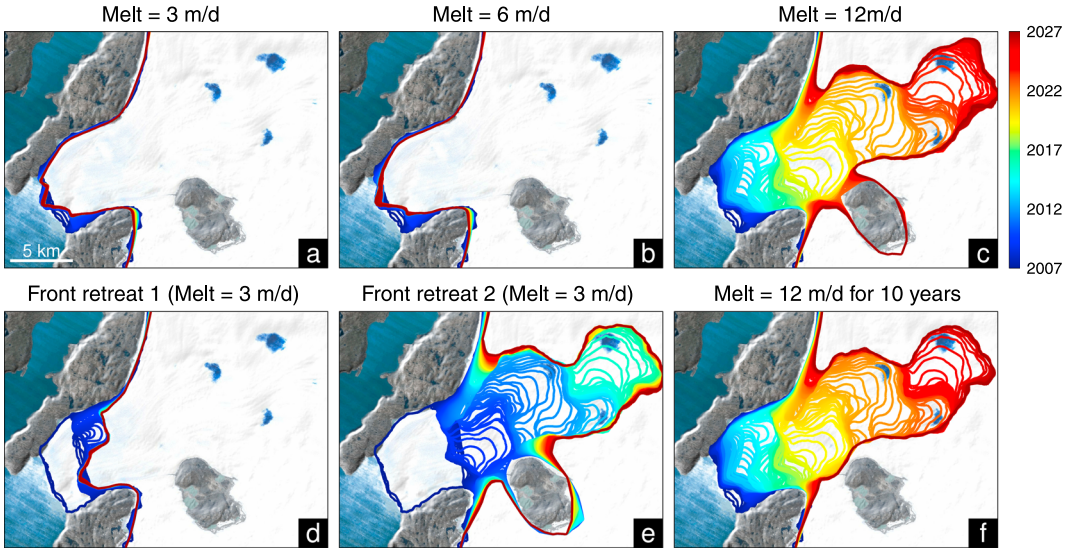

Figure 2. Modeled ice front positions of Store Gletscher between 2007 and 2027 under different scenarios overlaid on a Google Earth image (Landsat). (a) maximum summer melt of 3 m/d, (b) maximum summer melt of 6 m/d, (c) maximum summer melt of 12 m/d, (d) initial ice front retreat of 4 km with a maximum summer melt of 3 m/d, (e) initial ice front retreat of 8 km with a maximum summer melt of 3 m/d, and (f) maximum summer melt of 12 m/d for 10 years and then 3 m/d.

further inland during the summer months but readvances to its initial position in the winter. The velocity also remains stable similarly to the unperturbed experiment, and the model only loses about 3% of its initial volume (i.e., within the model boundary, excluding the ice volume from the rest of the drainage basin). In order to get a significant response of the glacier over 20 years, the applied melt rate needs to reach 12 m/d in the summer (Figures 2c and 3c). We see that the velocity doubles, and the ice front retreats 5 km upstream, toward the back of the sill, over the first 7 years of the run, and remains stable along the northern side of the fjord but continues to retreat along the southern half, where the bed is deepest (Movie S3). This retreat ends up destabilizing the northern side of the ice front, and the front continues to retreat dramatically another 20 km upstream of the initial position and stabilizes during the last year of the simulation. The velocities remain high, in the 10 km/yr range or twice higher than the present day velocities, throughout the simulation. After 20 years, the glacier has lost 234 km^3, or 36% of the model initial volume. We also notice (Figure 2c) that the ice stream is split into two distinct branches around a nunatak at the end of the simulation, which is a significant advantage of the implicit method used here, as an explicit method would have required complex operations on the set of segments.

This simulation suggests that the glacier starts to retreat quickly inland once it detaches from its sills, as it retreats faster in the large overdeepening upstream of this sill (Movie S3). To test this hypothesis, we run two additional simulations where the model initial ice front position is 4 and 8 km upstream of its current position while keeping our reference melt rate of 3 m/d (Figures 2d, 2e, 3d, and 3e and Movies S4 and S5). The 4 km retreat coincides with the location of a ridge along the northern side of the fjord toward the back of the sill, and the 8 km retreat coincides with the beginning of the reverse bed. For an initial retreat of 4 km, the front remains stable in the vicinity of the retreated position, i.e., does not advance or retreat on average (Figures 2d and 3d). In terms of velocity, the model responds instantly by a strong increase in velocity near the ice front to almost 10 km/yr, and this acceleration propagates up to 30 km upstream. The velocities return close to their initial values after about 6 years and remain stable for the rest of the run. The glacier loses about 13% of its ice over 20 years.

The 8 km retreat experiment (Figures 2e and 3e and Movie S5), on the other hand, leads to a strong retreat of Store. The ice front remains somewhat stable around its initial retreated position for about 5 years, toward the back of the sill, and then retreats and stabilizes another 15 km upstream, in a similar position as for the 12 m/d melting experiment (Figure 2c), just upstream of the three blue supraglacial lakes visible in the Landsat image. The velocities respond instantly to the initial retreat, and the glacier slows down over the first 5 years,

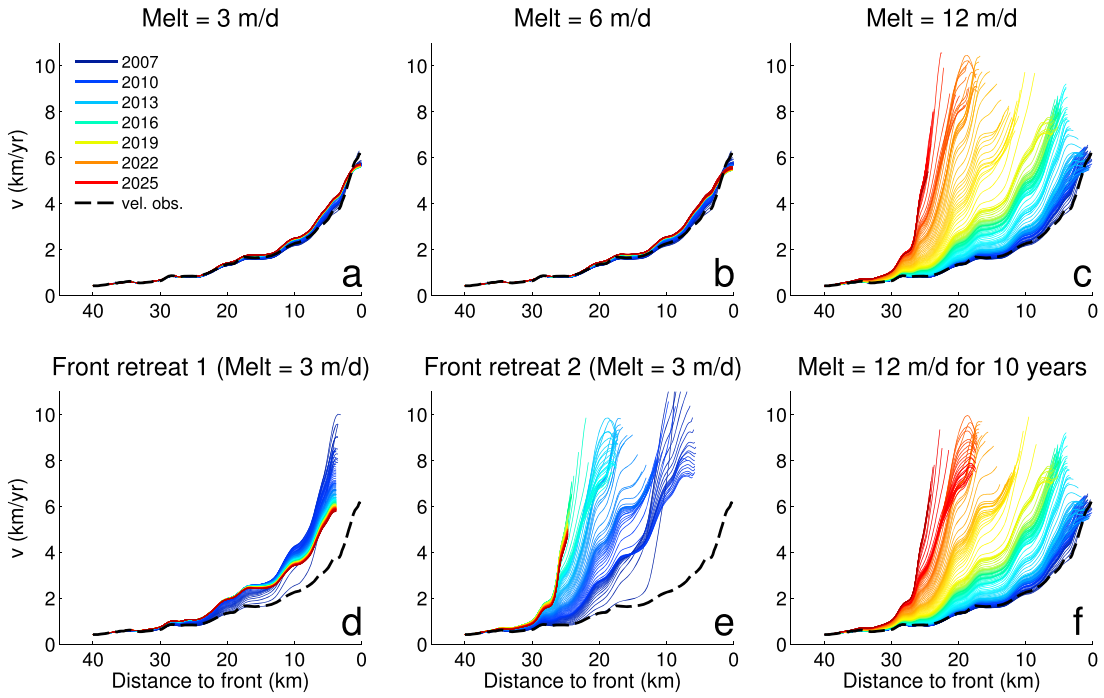

Figure 3. Modeled ice velocity of Store Gletscher along its center line (see Figure 1b) between 2007 and 2027 under different scenarios. The black dashed line shows the 2007 observed velocity. (a) maximum summer melt of 3 m/d, (b) maximum summer melt of 6 m/d, (c) maximum summer melt of 12 m/d, (d) initial ice front retreat of 4 km with a maximum summer melt of 3 m/d, (e) initial ice front retreat of 8 km with a maximum summer melt of 3 m/d, and (f) maximum summer melt of 12 m/d for 10 years and then 3 m/d.

until the ice front starts to retreat again and leads to another phase of acceleration of the glacier, which then stabilizes at a velocity of about 5 km/yr. At the end of the 20 year simulation, the glacier has lost 290 km^3 or 44% of the model initial volume.

An important aspect of the behavior of the glacier is its ability to return to its initial state after a temporary change in forcing. To investigate the reversible character of the glacier, we perform a final experiment where the melt rate is set as 12 m/d in the summer for 10 years and switched back to 3 m/d for the last 10 years of the simulation (Figures 2f and 3f and Movie S6). We see that the model does not return to its initial position after the high melt rates are turned off and continues to retreat until it finds another stabilizing feature in the bed topography, which is consistent with our initial retreat experiments. In other words, once the ice front detaches from its sill and enters the overdeepening, it starts an irreversible retreat regardless of the applied melt rate at the front.

4. Discussion

The unperturbed experiment (Figures 2a and 3a) shows that our model is in good agreement with observations in terms of current ice front position and its stability. The modeled velocity of Store is also in excellent agreement with measurements and remains stable over the 20 year run.

Our experiments suggest that Store is in a remarkably stable state and is not affected by larger melt rates, neither in terms of ice front dynamics nor in terms of velocities for our 20 year simulations. In order to trigger a retreat of the glacier, we need to quadruple the melt rate to a maximum summer melt of 12 m/d. This amount of melt would require, e.g., an increase of 7°C in ocean thermal forcing, with a quadrupling of the subglacial water discharge [*Xu et al.*, 2013]. For melt rates lower than 12 m/d, the glacier readvances in the winter over its sill and recovers from its summer retreat. For higher melt rates, the ice front does not fully recover in the winter and retreats slowly summer after summer until it detaches from its sill and starts an unstoppable retreat (Movie S3).

The fact that a moderate change in the melt at the calving face of Store has very little influence on its position or its dynamics, as long as it remains below 12 m/d in the summer, is in agreement with a previous study based

on a 2-D flowband model [*Todd and Christoffersen*, 2014] that showed that the glacier is not strongly sensitive to ocean forcing.

All of these experiments and particularly the two additional experiments, for which we keep the melt rates at their reference value of 3 m/d but start with a retreated position of the calving front, demonstrate that the bed topography dictates the stable positions of the calving front and the regions where we have fast retreat rates.

Since the bed topography controls the locations where glacier ice fronts can be stable, it is therefore critical to have the best description of the bed topography to understand glacier behavior. The same experiments using the bed topography of *Bamber et al.* [2013] would have yielded completely different results, as the sill is above sea level in their map. This control on ice front dynamics could also explain why different outlet glaciers, even within the same fjord system, respond differently to a change in ocean circulation or amount of runoff [*Moon and Joughin*, 2008; *McFadden et al.*, 2011] because of differences in bed topography.

Our model also shows that the ice front dynamics needs to be plan view or 3-D to account for the complex topography of Greenland fjords. In the strong melt experiments (Figures 2c and 2f), the ice front of the northern half of the ice stream stabilizes in the vicinity of a ridge parallel to the flow direction (Figure 1b). This ridge does not go across the ice stream, and the southern half of the ice stream is not stabilized by the ridge and ends up destabilizing the entire ice stream. In a flow line model or vertical flowband model, depending on where the flow line is located, the ice front might either be stable or not depending on the bed topography of this specific flow line. It is therefore critical that a model includes a comprehensive representation of the bed topography in order to accurately capture the dynamics of the ice front.

In terms of model limitations, we did not account here for the presence of sea ice and mélange in the vicinity of the calving front, and it has been shown that they could have an impact on ice front dynamics [*Amundson et al.*, 2010; *Todd and Christoffersen*, 2014]. We also need to further validate our calving criterion (equation (4)) by applying the same approach to a glacier for which we have a record of retreat and also quality bed topography data. Additionally, these results are based on a Shelfy-Stream Approximation, which also has limitations even though it is a very good approximation for outlet glaciers. Finally, errors in bed topography might also alter our results, despite the fact that Store is one of the few glaciers in Greenland for which we have quality bed and bathymetry data. More details in the bed topography could provide additional anchor points for the ice front and intermediary stable positions.

The methodology presented here can be applied broadly to other glaciers in Greenland and Antarctica. By modeling the response of marine terminating glaciers to enhanced melting at the submerged calving face, it is possible to assess the degree of vulnerability of individual glaciers to ocean-induced melt and quantify the impact of ice-ocean interactions and calving on glacier flow.

5. Conclusion

We employ the level set method to track moving boundaries within a 2-D plan view ice sheet model. We introduce a novel calving law derived from the von Mises yield criterion and apply it to investigate the response of Store Gletscher to enhanced melt rate at its calving face. We find that Store is remarkably stable due to the sill where its ice front is currently sitting, but we also show that if the ice front retreats inland and detaches from its sill, because of a quadrupling in melt rate, the ice front will start a long phase of retreat that cannot be stopped even if the melt rates are switched back to zero. After 20 years, the glacier stabilizes 27 km upstream where the bed raises above sea level. If ice-ocean interactions are the triggering mechanism of ice front retreat, bed topography is the main control on how far the ice front retreats for a given perturbation. It is therefore critical to have an accurate representation of the bed topography to interpret glacier behavior. The sensitivity of ice front dynamics to bed topography may explain the variability in the response of Greenland outlet glaciers to warmer ocean currents.

Acknowledgments
This work was performed at the Department of Earth System Science, University of California, Irvine, under a contract with the National Aeronautics and Space Administration, Cryospheric Sciences Program, grant NNX15AD55G.

References

Albrecht, T., and A. Levermann (2014), Fracture-induced softening for large-scale ice dynamics, *Cryosphere*, *8*(2), 587–605, doi:10.5194/tc-8-587-2014.

Albrecht, T., M. Martin, M. Haseloff, R. Winkelmann, and A. Levermann (2011), Parameterization for subgrid-scale motion of ice-shelf calving fronts, *Cryosphere*, *5*(1), 35–44, doi:10.5194/tc-5-35-2011.

Amundson, J. M., M. Fahnestock, M. Truffer, J. Brown, M. P. Lüthi, and R. J. Motyka (2010), Ice mélange dynamics and implications for terminus stability, Jakobshavn Isbræ, Greenland, *J. Geophys. Res.*, *115*, F01005, doi:10.1029/2009JF001405.

Bamber, J. L., et al. (2013), A new bed elevation dataset for Greenland, *Cryosphere*, *7*, 499–510, doi:10.5194/tc-7-499-2013.
Benn, D. I., C. R. Warren, and R. H. Mottram (2007), Calving processes and the dynamics of calving glaciers, *Earth Sci. Rev.*, *82*(3–4), 143–179, doi:10.1016/j.earscirev.2007.02.002.
Bondzio, J. H., H. Seroussi, M. Morlighem, T. Kleiner, M. Rückamp, A. Humbert, and E. Larour (2016), Modelling calving front dynamics using a level-set method: Application to Jakobshavn Isbræ, West Greenland, *Cryosphere*, *10*(2), 497–510, doi:10.5194/tc-10-497-2016.
Church, J., et al. (2013), *Sea Level Change*, book section 13, pp. 1137–1216, Cambridge Univ. Press, Cambridge, U. K., and New York, doi:10.1017/CBO9781107415324.026.
Cuffey, K., and W. S. B. Paterson (2010), *The Physics of Glaciers*, Elsevier, 4th ed., Elsevier, Oxford, U. K.
Howat, I. M., I. Joughin, M. Fahnestock, B. E. Smith, and T. A. Scambos (2008), Synchronous retreat and acceleration of southeast Greenland outlet glaciers 2000–06: Ice dynamics and coupling to climate, *J. Glaciol.*, *54*(187), 646–660.
Howat, I. M., A. Negrete, and B. E. Smith (2014), The Greenland Ice Mapping Project (GIMP) land classification and surface elevation datasets, *Cryosphere*, *8*(4), 1509–1518, doi:10.5194/tc-8-1509-2014.
Hubbard, A., H. Blatter, P. Nienow, D. Mair, and B. Hubbard (1998), Comparison of a three-dimensional model for glacier flow with field data from Haut Glacier d'Arolla, Switzerland, *J. Glaciol.*, *44*(147), 368–378.
Larour, E., H. Seroussi, M. Morlighem, and E. Rignot (2012), Continental scale, high order, high spatial resolution, ice sheet modeling using the Ice Sheet System Model (ISSM), *J. Geophys. Res.*, *117*, F01022, doi:10.1029/2011JF002140.
Levermann, A., T. Albrecht, R. Winkelmann, M. A. Martin, M. Haseloff, and I. Joughin (2012), Kinematic first-order calving law implies potential for abrupt ice-shelf retreat, *Cryosphere*, *6*, 273–286.
MacAyeal, D. (1989), Large-scale ice flow over a viscous basal sediment: Theory and application to Ice Stream B, Antarctica, *J. Geophys. Res.*, *94*(B4), 4071–4087.
McFadden, E., I. Howat, I. Joughin, B. Smith, and Y. Ahn (2011), Changes in the dynamics of marine terminating outlet glaciers in West Greenland (2000–2009), *J. Glaciol.*, *116*, 1–16, doi:10.1029/2010JF001757.
Moon, T., and I. Joughin (2008), Changes in ice front position on Greenland's outlet glaciers from 1992 to 2007, *J. Geophys. Res.*, *113*, F02022, doi:10.1029/2007JF000927.
Morlighem, M., E. Rignot, H. Seroussi, E. Larour, H. Ben Dhia, and D. Aubry (2010), Spatial patterns of basal drag inferred using control methods from a full-Stokes and simpler models for Pine Island Glacier, West Antarctica, *Geophys. Res. Lett.*, *37*, L14502, doi:10.1029/2010GL043853.
Morlighem, M., E. Rignot, H. Seroussi, E. Larour, H. Ben Dhia, and D. Aubry (2011), A mass conservation approach for mapping glacier ice thickness, *Geophys. Res. Lett.*, *38*, L19503, doi:10.1029/2011GL048659.
Morlighem, M., H. Seroussi, E. Larour, and E. Rignot (2013), Inversion of basal friction in Antarctica using exact and incomplete adjoints of a higher-order model, *J. Geophys. Res. Earth Surf.*, *118*, 1746–1753, doi:10.1002/jgrf.20125.
Morlighem, M., E. Rignot, J. Mouginot, H. Seroussi, and E. Larour (2014), High-resolution ice thickness mapping in South Greenland, *Ann. Glaciol.*, *55*(67), 64–70, doi:10.3189/2014AoG67A088.
Nick, F. M., A. Vieli, M. L. Andersen, I. Joughin, A. Payne, T. L. Edwards, F. Pattyn, and R. S. W. van de Wal (2013), Future sea-level rise from Greenland's main outlet glaciers in a warming climate, *Nature*, *497*(7448), 235–238.
Osher, S., and J. Sethian (1988), Fronts propagating with curvature-dependent speed: Algorithms based on Hamilton-Jacobi formulations, *J. Comput. Phys.*, *79*(1), 12–49.
Petrovic, J. (2003), Review mechanical properties of ice and snow, *J. Mater. Sci.*, *38*(1), 1–6, doi:10.1023/A:1021134128038.
Pollard, D., and R. DeConto (2009), Modelling West Antarctica ice sheet growth and collapse through the past five million years, *Nature*, *458*, 329–332.
Rignot, E., and J. Mouginot (2012), Ice flow in Greenland for the International Polar Year 2008–2009, *Geophys. Res. Lett.*, *39*, L11501, doi:10.1029/2012GL051634.
Rignot, E., I. Fenty, Y. Xu, C. Cai, and C. Kemp (2015), Undercutting of marine-terminating glaciers in West Greenland, *Geophys. Res. Lett.*, *42*, 5909–5917, doi:10.1002/2015GL064236.
Seroussi, H., M. Morlighem, E. Rignot, A. Khazendar, E. Larour, and J. Mouginot (2013), Dependence of century-scale projections of the Greenland ice sheet on its thermal regime, *J. Glaciol.*, *59*(218), 1024–1034, doi:10.3189/2013JoG13J054.
Todd, J., and P. Christoffersen (2014), Are seasonal calving dynamics forced by buttressing from ice mélange or undercutting by melting? Outcomes from full-stokes simulations of Store Glacier, West Greenland, *Cryosphere*, *8*(6), 2353–2365, doi:10.5194/tc-8-2353-2014.
van Angelen, J. H., M. R. van den Broeke, B. Wouters, and J. T. M. Lenaerts (2014), Contemporary (1960–2012) evolution of the climate and surface mass balance of the Greenland ice sheet, *Surv. Geophys.*, *35*(5), 1155–1174, doi:10.1007/s10712-013-9261-z.
van den Broeke, M., J. Bamber, J. Ettema, E. Rignot, E. Schrama, W. J. van de Berg, E. van Meijgaard, I. Velicogna, and B. Wouters (2009), Partitioning recent Greenland mass loss, *Science*, *326*(5955), 984–986, doi:10.1126/science.1178176.
Vaughan, D. (1993), Relating the occurence of crevasses to surface strain rates, *J. Glaciol.*, *39*(132), 255–266.
Weidick, A. (1968), *Observations on Some Holocene Glacier Fluctuations in West Greenland*, C. A. Reitzel, illus., 1 map, 1 loose leaf of plate, 1 loose leaf of map. ; 27 cm, 203 pp., Copenhagen.
Weidick, A., and O. Bennike (2007), *Quaternary Glaciation History and Glaciology of Jakobshavn Isbrae and the Disko Bugt Region, West Greenland: A Review*, Geol. Surv., ill. (chiefly col.), maps ; 28 cm, 78 pp., Copenhagen.
Xu, Y., E. Rignot, I. Fenty, D. Menemenlis, and M. M. Flexas (2013), Subaqueous melting of Store Glacier, West Greenland from three-dimensional, high-resolution numerical modeling and ocean observations, *Geophys. Res. Lett.*, *40*, 4648–4653, doi:10.1002/grl.50825.